Acta Crystallographica Section F
Structural Biology and Crystallization Communications
ISSN 1744-3091
Editors: **H. M. Einspahr and M. S. Weiss**

Expression, purification, crystallization and preliminary X-ray structure analysis of *Vibrio cholerae* uridine phosphorylase in complex with thymidine

Alexander A. Lashkov, Azat G. Gabdulkhakov, Igor I. Prokofev, Tatyana A. Seregina, Sergey E. Sotnichenko, Andrey V. Lyashenko, Alexander A. Shtil, Alexander S. Mironov, Christian Betzel and Al'bert M. Mikhailov

Acta Cryst. (2012). F**68**, 1394–1397

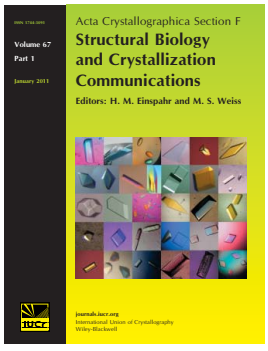

Acta Crystallographica Section F
Structural Biology and Crystallization Communications
ISSN 1744-3091

Expression, purification, crystallization and preliminary X-ray structure analysis of *Vibrio cholerae* uridine phosphorylase in complex with thymidine

Alexander A. Lashkov,[a] Azat G. Gabdulkhakov,[a] Igor I. Prokofev,[a] Tatyana A. Seregina,[a,b] Sergey E. Sotnichenko,[a] Andrey V. Lyashenko,[a] Alexander A. Shtil,[c] Alexander S. Mironov,[b] Christian Betzel[d] and Al'bert M. Mikhailov[a]*

[a]A. V. Shubnikov Institute of Crystallography, Russian Academy of Sciences, Leninsky Prospect 59, Moscow 119333, Russian Federation, [b]State Research Institute of Genetics and Selection of Industrial Microorganisms, 1st Dorozhny Proezd 1, Moscow 117545, Russian Federation, [c]Blokhin Cancer Center, Kashirskoye Shosse 24, Moscow 115478, Russian Federation, and [d]University of Hamburg, Notkestrasse 85, 22603 Hamburg, Germany

Correspondence e-mail: amm@ns.crys.ras.ru

Received 3 September 2012
Accepted 2 October 2012

A high-resolution structure of the complex of *Vibrio cholerae* uridine phosphorylase (*Vch*UPh) with its physiological ligand thymidine is important in order to determine the mechanism of the substrate specificity of the enzyme and for the rational design of pharmacological modulators. Here, the expression and purification of *Vch*UPh and the crystallization of its complex with thymidine are reported. Conditions for crystallization were determined with an automated Cartesian Dispensing System using The Classics, MbClass and MbClass II Suites crystallization kits. Crystals of the *Vch*UPh–thymidine complex (of dimensions ~200–350 µm) were grown by the sitting-drop vapour-diffusion method in ~7 d at 291 K. The crystallization solution consisted of 1.5 µl *Vch*UPh (15 mg ml^{-1}), 1 µl 0.1 *M* thymidine and 1.5 µl reservoir solution [15%(*w*/*v*) PEG 4000, 0.2 *M* $MgCl_2.6H_2O$ in 0.1 *M* Tris–HCl pH 8.5]. The crystals diffracted to 2.12 Å resolution and belonged to space group $P2_1$ (No. 4), with unit-cell parameters a = 91.80, b = 95.91, c = 91.89 Å, β = 119.96°. The Matthews coefficient was calculated as 2.18 Å^3 Da^{-1}; the corresponding solvent content was 43.74%.

1. Introduction

Uridine phosphorylase (UPh; EC 2.4.2.3) is a major enzyme that catalyzes the phosphorylation of pyrimidine nucleotides (Pizzorno *et al.*, 1998, 2002; Schwartz *et al.*, 1985). The activity of UPh is known to be vital in some pathogenic bacteria and protozoa (Jiménez *et al.*, 1989; Lee *et al.*, 1988). In previous publications, we have reported structures of UPh from *Salmonella typhimurium* with physiological ligands and pharmacological inhibitors (Dontsova *et al.*, 2004, 2005; Timofeev *et al.*, 2007; Lashkov *et al.*, 2009, 2010, 2012). However, the diffraction resolution of complexes of bacterial UPh with thymidine does not allow conclusions to be drawn regarding the details of enzyme–ligand binding. Based on structural and biochemical data on *Escherichia coli* UPh (*Ec*UPh), a mechanism of substrate specificity has been proposed (Caradoc-Davies *et al.*, 2004; PDB entry 1rxu; 3.1 Å resolution). The higher affinity of *Ec*UPh for uridine compared with that for thymidine has been attributed to the formation of hydrogen bonds between the hydroxyl group at the 2′ position of the ribose ring of uridine and the carboxy group of the Glu198 side chain in the active centre of the enzyme. Thymidine lacks the hydroxyl group at the 2′ position of the ribose ring. Furthermore, a lower affinity of *Ec*UPh for thymidine than for uridine may also be explained by steric hindrance caused by the methyl group at position 5 of thymidine (Caradoc-Davies *et al.*, 2004). However, even bulkier (compared with the methyl group) hydrophobic substituents at position 5 of the pyrimidine ring do not hamper the binding of ligands to *Ec*UPh (Bu *et al.*, 2005; Drabikowska, Lissowska, Draminski *et al.*, 1987; Drabikowska, Lissowska, Veres *et al.*, 1987; Niedzwicki *et al.*, 1982; Pizzorno *et al.*, 1998; Veres *et al.*, 1987). Overall, it is difficult to unequivocally predict the interaction of individual chemical groups with *Ec*UPh on the basis of the structure of the *Ec*UPh–thymidine complex refined at 3.1 Å resolution (Caradoc-Davies *et al.*, 2004). A higher resolution structure of the complex is needed. From the biomedical viewpoint, data on the three-dimensional structures of UPh–thymidine complexes will be beneficial for the design of novel pyrimidine-based drugs.

In this study, we analyzed the structure of the complex formed by *Vibrio cholerae* UPh (*Vch*UPh) with thymidine.

2. Expression

2.1. Cloning the *V. cholerae udp* gene into pUC19 vector

The primers 5′-CC*GGATCC*GCGCCACATCAAGTGGCGC-3′ (forward) and 5′-GGG*GAATTC*AAGTAGGAAGGGGATAGA-GG-3′ (reverse) were selected on the basis of the complete sequence of the *V. cholerae* genome (GenBank accession No. CAB94933.1). These primers were utilized for PCR amplification of the *udp* gene coding for *Vch*UPh using *V. cholerae* chromosomal DNA as a template. The PCR product included regulatory and structural regions of the *udp* gene and *Eco*RI and *Bam*HI recognition sites (italicized). The amplified DNA fragment was eluted from agarose gel using GeneClean (Fermentas, Lithuania), digested with *Eco*RI and *Bam*HI and cloned into a multiple-copy vector pUC19 (Ap^r, *lacZ* M15, pBR322 ori). The resulting construct pMZ21 (pUC19 with a 1030 bp *Eco*RI–*Bam*HI fragment of the *V. cholerae udp* gene) was used for transformation of *E. coli* AM201 strain (genotype *supE hsdD5 thi* Δ*(lac–proAB)* Δ*metE-udp*/F′ [*traD36 proAB*$^{(+)}$ *lacI*$^{(q)}$ *lacZ* Δ*M15*]) followed by selection of $Amp^R Udp^+$ clones (Zolotukhina *et al.*, 2003). After selection of the *E. coli* transformants, the plasmid DNA was isolated and sequenced. The DNA encoded by pMZ21 carried one full reading frame for a 253-amino-acid protein with a predicted molecular mass of 27.5 kDa (Zolotukhina *et al.*, 2003).

2.2. Expression of the *udp* gene in *E. coli*

E. coli strain AM201 containing the pMZ21 plasmid was grown overnight in enriched Luria broth supplemented with 100 µg ml^{-1} ampicillin. Cells were pelleted, resuspended in buffer (62.5 m*M* Tris–HCl pH 6.8, 5% glycerol, 2% β-mercaptoethanol, 0.1% sodium dodecyl sulfate) and then boiled for 10 min. Proteins were resolved by SDS–PAGE. Proteins of the *E. coli* AM201 strain carrying an empty pUC19 plasmid were used as a control. An ∼28 kDa band corresponding to the *udp* gene product was detectable (Fig. 1). The molecular mass of the expressed protein was close to the predicted value (27.5 kDa) calculated on the basis of *udp* gene sequencing (Zolotukhina *et al.*, 2003).

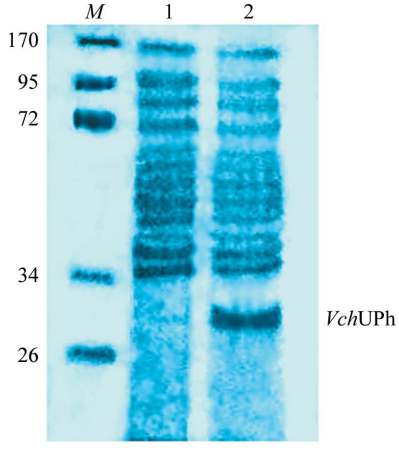

Figure 1
SDS–PAGE of extracts of *E. coli* AM201 strains transformed with empty pUC19 plasmid (lane 1) or pMZ21 plasmid carrying a 1030 bp fragment of the *udp* gene coding for *Vch*UPh (lane 2). The position of the band corresponding to *Vch*UPh is indicated. Lane *M*, protein molecular-mass markers (labelled in kDa).

3. Purification

To purify *Vch*UPh, *E. coli* AM201 strain carrying the pMZ21 plasmid was grown in Luria broth with 100 µg ml^{-1} ampicillin on a shaker (250 rev min^{-1}; 310 K) for 12 h. The bacterial cells were pelleted. The yield was 9 g per 1.5 l of growth medium. The cells were resuspended in 50 m*M* Tris–HCl buffer pH 7.5, 5 m*M* β-mercaptoethanol, 0.3 m*M* phenylmethanesulfonyl fluoride (PMSF) and disrupted using ultrasound. After centrifugation, the supernatant was diluted with a 10%(*v*/*v*) solution of Polymin P (pH 6.0) and the mixture was stirred for 12 h at 277 K. The pellet was resuspended in a buffer consisting of 50 m*M* Tris–HCl pH 7.5, 2 *M* ammonium sulfate, 5 m*M* β-mercaptoethanol, 0.3 m*M* PMSF and incubated for 12 h at 277 K. The pellet was concentrated by low-speed centrifugation, resuspended in 50 m*M* Tris–HCl pH 7.5, 2 *M* ammonium sulfate and loaded onto a Butyl-Sepharose column (Amersham Pharmacia Biotech) equilibrated with the same buffer. The protein was eluted with a gradient of ammonium sulfate from 2 to 0 *M* at a flow rate of 0.5 ml min^{-1}. Fractions pooled after column purification were analyzed by SDS–PAGE under denaturing conditions (Fig. 2). In the second step of protein purification, the pooled fractions containing *Vch*UPh were dialyzed against 50 m*M* Tris–HCl pH 7.5, 20 m*M* NaCl and loaded onto a Q-Sepharose column equilibrated with the same buffer. The enzyme was eluted using an NaCl gradient from 20 m*M* to 1 *M* at a flow rate of 1 ml min^{-1}. The fractions were pooled, resolved on SDS–PAGE under denaturing conditions (Fig. 2), centrifuged, dialyzed against buffer (20 m*M* Tris–HCl pH 7.5, 20 m*M* NaCl) and concentrated to 15 mg ml^{-1} in the same buffer solution.

4. Crystallization

The conditions for crystallization of the complexes of *Vch*UPh with thymidine were determined using an automated Cartesian Dispensing System (Genomic Solutions; http://www.digilabglobal.com) using The Classics, MbClass and MbClass II Suites crystallization kits (Qiagen). Crystals of the *Vch*UPh–thymidine complex with dimensions of ∼200–350 µm were grown in 7 d using the sitting-drop vapour-diffusion method at 291 K (Fig. 3). The crystallization mixture consisted of 1.5 µl protein solution (15 mg ml^{-1}), 1.5 µl reservoir solution and 1 µl 0.1 *M* thymidine. The reservoir solution consisted of 0.2 *M* $MgCl_2.6H_2O$, 15%(*w*/*v*) polyethylene glycol (PEG) 4000 in 0.1 *M* Tris–HCl pH 8.5.

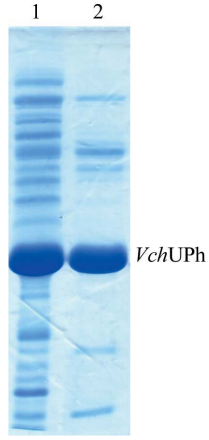

Figure 2
SDS–PAGE analysis of the *Vch*UPh fractions after separation on Butyl-Sepharose (lane 1) and Q-Sepharose (lane 2).

5. X-ray data collection and preliminary X-ray structure analysis

The crystal was directly flash-cooled in a stream of nitrogen gas at 100 K using an Oxford Cryosystems cooling device. Prior to freezing in liquid nitrogen, the crystal was transferred into a cryoprotectant solution [0.2 *M* $MgCl_2.6H_2O$, 15%(*w*/*v*) PEG 4000, 40%(*w*/*v*) PEG 400 in 0.1 *M* Tris–HCl pH 8.5]. X-ray diffraction data were collected from the *Vch*UPh–thymidine complex crystal on the X13 Consortium Beamline at DORIS, DESY, Hamburg, Germany using a MAR CCD 165 detector (MAR Research, Germany) with a crystal-to-detector distance of 201 mm. The wavelength was 0.801 Å and each frame was exposed for 30 s. All data were indexed, merged and processed using *XDS* (Kabsch, 2010), *POINTLESS* and *SCALA* (Winn *et al.*, 2011). The data statistics are summarized in Table 1.

For phasing, molecular replacement was applied using the program *Phaser* (McCoy *et al.*, 2007), with the structure of *Vch*UPh (PDB entry 3o6v; Center for Structural Genomics of Infectious Diseases, unpublished work) as a model after the removal of all ligands including water molecules.

The best solution was found for three homodimers in the asymmetric unit forming one hexameric molecule. The starting *R* factor was 0.395 and the overall correlation coefficient was 0.727. The Matthews coefficient was calculated to be 2.18 $Å^3$ Da^{-1} (Matthews, 1968), corresponding to 43.74% solvent content (Table 1). The initial model was confirmed by rigid-body refinement with *REFMAC* (Murshudov *et al.*, 2011). The program *Coot* (Emsley & Cowtan, 2004; Emsley *et al.*, 2010) was used to model the *Vch*UPh–thymidine complex. Further refinement was performed using restrained refinement in *REFMAC* (Murshudov *et al.*, 2011). The structure of the *Vch*UPh–thymidine complex was characterized by an R_{work} of 0.2220 and an R_{free} of 0.2888.

Analysis of difference electron-density maps calculated with coefficients ($|F_{obs}| - |F_{calc}|$) in *Coot* (Emsley & Cowtan, 2004; Emsley *et al.*, 2010) identified the position of the thymidine molecule in the active centre of *Vch*UPh (Fig. 4). Refinement of the *Vch*UPh–thymidine complex is currently in progress and will be published elsewhere.

This initial report of the structure of the complex of *Vch*UPh with its physiological ligand thymidine provides a structural basis for the prediction of the inhibitory potency of newly designed antagonists of this enzyme.

Table 1
Statistics of data collection and processing.

Values in parentheses are for the highest resolution shell.

Space group	$P2_1$ [No. 4]
Unit-cell parameters (Å, °)	a = 91.80, b = 95.91, c = 91.89, β = 119.96
Radiation source	X13, DORIS, DESY, Hamburg, Germany
Wavelength (Å)	0.801
Temperature (K)	100
Detector	MAR CCD 165
Oscillation range (°)	1.0
No. of frames	360
Resolution range (Å)	29.69–2.12 (2.23–2.12)
Mosaicity (°)	0.2
Total reflections	597573 (80251)
Total independent reflections	78327 (11334)
R_{merge}†	0.082 (0.247)
Average $I/\sigma(I)$	22.8 (7.6)
Average multiplicity	7.6 (7.1)
Completeness (%)	99.8 (99.0)
V_M ($Å^3$ Da^{-1})	2.18
Solvent content (%)	43.74

† $R_{merge} = \sum_{hkl}\sum_i |I_i(hkl) - \langle I(hkl)\rangle| / \sum_{hkl}\sum_i I_i(hkl)$, where $I_i(hkl)$ is the intensity of the the ith measurement of reflection hkl and $\langle I(hkl)\rangle$ is the average intensity of reflection hkl.

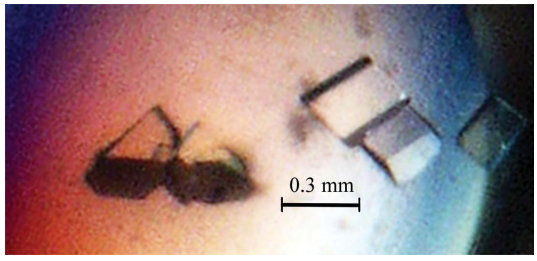

Figure 3
Crystals of *Vch*UPh.

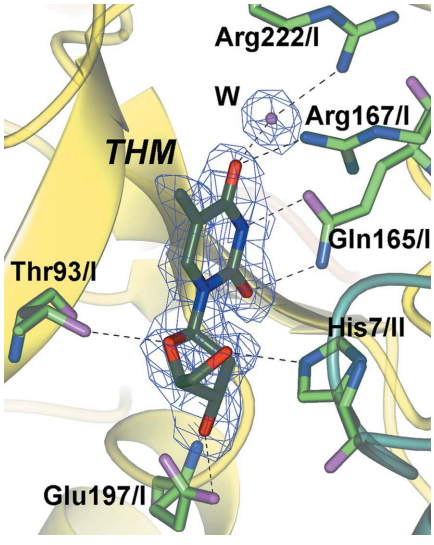

Figure 4
The binding site of *Vch*UPh complexed with thymidine (prepared using *CCP4mg*; McNicholas *et al.*, 2011). Difference electron-density maps around the ligands were calculated with coefficients ($2|F_{obs}| - |F_{calc}|$). Residues Glu196/I, Thr93/I, Arg222/I, Arg167/I, Gln165/I belong to subunit I and His7/II belongs to subunit II. Water and thymidine are labelled W and THM, respectively.

This study was supported by the funding budget of A. V. Shubnikov Institute of Crystallography and by State Contract No. 16.512.11.2235.

References

Bu, W., Settembre, E. C., el Kouni, M. H. & Ealick, S. E. (2005). *Acta Cryst.* D**61**, 863–872.
Caradoc-Davies, T. T., Cutfield, S. M., Lamont, I. L. & Cutfield, J. F. (2004). *J. Mol. Biol.* **337**, 337–354.
Dontsova, M. V., Gabdoulkhakov, A. G., Molchan, O. K., Lashkov, A. A., Garber, M. B., Mironov, A. S., Zhukhlistova, N. E., Morgunova, E. Y., Voelter, W., Betzel, C., Zhang, Y., Ealick, S. E. & Mikhailov, A. M. (2005). *Acta Cryst.* F**61**, 337–340.
Dontsova, M. V., Savochkina, Y. A., Gabdoulkhakov, A. G., Baidakov, S. N., Lyashenko, A. V., Zolotukhina, M., Errais Lopes, L., Garber, M. B., Morgunova, E. Y., Nikonov, S. V., Mironov, A. S., Ealick, S. E. & Mikhailov, A. M. (2004). *Acta Cryst.* D**60**, 709–711.
Drabikowska, A. K., Lissowska, L., Draminski, M., Zgit-Wroblewska, A. & Shugar, D. (1987). *Z. Naturforsch. C*, **42**, 288–296.
Drabikowska, A. K., Lissowska, L., Veres, Z. & Shugar, D. (1987). *Biochem. Pharmacol.* **36**, 4125–4128.
Emsley, P. & Cowtan, K. (2004). *Acta Cryst.* D**60**, 2126–2132.

Emsley, P., Lohkamp, B., Scott, W. G. & Cowtan, K. (2010). *Acta Cryst.* D**66**, 486–501.
Jiménez, B. M., Kranz, P., Lee, C. S., Gero, A. M. & O'Sullivan, W. J. (1989). *Biochem. Pharmacol.* **38**, 3785–3789.
Kabsch, W. (2010). *Acta Cryst.* D**66**, 125–132.
Lashkov, A. A., Gabdoulkhakov, A. G., Shtil, A. A. & Mikhailov, A. M. (2009). *Acta Cryst.* F**65**, 601–603.
Lashkov, A. A., Sotnichenko, S. E., Prokofiev, I. I., Gabdulkhakov, A. G., Agapov, I. I., Shtil, A. A., Betzel, C., Mironov, A. S. & Mikhailov, A. M. (2012). *Acta Cryst.* D**68**, 968–974.
Lashkov, A. A., Zhukhlistova, N. E., Gabdoulkhakov, A. H., Shtil, A. A., Efremov, R. G., Betzel, C. & Mikhailov, A. M. (2010). *Acta Cryst.* D**66**, 51–60.
Lee, C. S., Jiménez, B. M. & O'Sullivan, W. J. (1988). *Mol. Biochem. Parasitol.* **30**, 271–277.
Matthews, B. W. (1968). *J. Mol. Biol.* **33**, 491–497.
McCoy, A. J., Grosse-Kunstleve, R. W., Adams, P. D., Winn, M. D., Storoni, L. C. & Read, R. J. (2007). *J. Appl. Cryst.* **40**, 658–674.
McNicholas, S., Potterton, E., Wilson, K. S. & Noble, M. E. M. (2011). *Acta Cryst.* D**67**, 386–394.
Murshudov, G. N., Skubák, P., Lebedev, A. A., Pannu, N. S., Steiner, R. A., Nicholls, R. A., Winn, M. D., Long, F. & Vagin, A. A. (2011). *Acta Cryst.* D**67**, 355–367.
Niedzwicki, J. G., Chu, S. H., el Kouni, M. H., Rowe, E. C. & Cha, S. (1982). *Biochem. Pharmacol.* **31**, 1857–1861.
Pizzorno, G., Cao, D., Leffert, J. J., Russell, R. L., Zhang, D. & Handschumacher, R. E. (2002). *Biochim. Biophys. Acta*, **1587**, 133–144.
Pizzorno, G., Yee, L., Burtness, B. A., Marsh, J. C., Darnowski, J. W., Chu, M. Y. Y., Chu, S. H., Chu, E., Leffert, J. J., Handschumacher, R. E. & Calabresi, P. (1998). *Clin. Cancer Res.* **4**, 1165–1175.
Schwartz, P. M., Moir, R. D., Hyde, C. M., Turek, P. J. & Handschumacher, R. E. (1985). *Biochem. Pharmacol.* **34**, 3585–3589.
Timofeev, V. I., Lashkov, A. A., Gabdoulkhakov, A. G., Pavlyuk, B. P., Kachalova, G. S., Betzel, C., Morgunova, E. Y., Zhukhlistova, N. E. & Mikhailov, A. M. (2007). *Acta Cryst.* F**63**, 852–854.
Veres, Z., Szinai, I., Szabolcs, A., Ujszászy, K. & Dénes, G. (1987). *Drugs Exp. Clin. Res.* **13**, 615–621.
Winn, M. D. *et al.* (2011). *Acta Cryst.* D**67**, 235–242.
Zolotukhina, M., Ovcharova, I., Eremina, S., Errais Lopes, L. & Mironov, A. S. (2003). *Res. Microbiol.* **154**, 510–520.